A novel *inhibitor of nuclear factor kappa-B kinase subunit gamma* mutation identified in an incontinentia pigmenti patient with syndromic tooth agenesis

Shichen Sun[a], Fang Li[a], Yang Liu[a], Hong Qu[b], Sing-Wai Wong[c], Li Zeng[a], Miao Yu[a], Hailan Feng[a], Haochen Liu[a,*], Dong Han[a,*]

[a] *Department of Prosthodontics, Peking University School and Hospital of Stomatology & National Clinical Research Center for Oral Diseases & National Engineering Laboratory for Digital and Material Technology of Stomatology & Beijing Key Laboratory of Digital Stomatology, 22 Zhongguancun South Avenue, Haidian District, Beijing 100081, PR China*
[b] *Center for Bioinformatics, State Key Laboratory of Protein and Plant Gene Research, College of Life Sciences, Peking University, Beijing 100871, PR China*
[c] *Oral and Craniofacial Biomedicine Curriculum, School of Dentistry, University of North Carolina at Chapel Hill, Chapel Hill, NC, USA*

ARTICLE INFO

ABSTRACT

Objective: To explore the gene mutation in an incontinentia pigmenti (IP) patient with syndromic tooth agenesis.

Methods: Long-range polymerase chain reaction (PCR) and Sanger sequencing were used to detect *inhibitor of nuclear factor kappa-B kinase subunit gamma* (*IKBKG*) mutation in the IP patient. We used the nuclear factor kappa B (NF-κB) reporter gene to assess activation of NF-κB, after transfecting an empty vector, wild-type, or mutant NF-κB essential modulator (NEMO) plasmid into *IKBKG*-deficient HEK293T cells, respectively. Furthermore, we performed immunoprecipitation and immunoblotting to describe the polyubiquitination of NEMO. Lastly, we detected the interactions between mutant NEMO and I kappa B kinase alpha (IKKα), I kappa B kinase beta (IKKβ), TNF receptor associated factor 6 (TRAF6), HOIL-1-interacting protein (HOIP), hemo-oxidized iron regulatory protein 2 ligase 1 (HOIL-1), and SHANK-associated RH domain interactor (SHARPIN).

Results: A *de novo* nonsense mutation in *IKBKG* (c.924C > G; p.Tyr308*) was observed. The Tyr308* mutation inhibited activation of the NF-κB pathway by reducing K63-linked polyubiquitination and linear polyubiquitination. The mutant NEMO was not able to interact with TRAF6, HOIL-1, or SHARPIN.

Conclusions: We identified a novel nonsense *IKBKG* mutation (c.924C > G; p.Tyr308*) in an IP patient with syndromic tooth agenesis. This research enriches the mutation spectrum of the *IKBKG* gene.

1. Introduction

Tooth agenesis is defined as the developmental absence of one or more teeth (excluding the third molars). The prevalence of tooth agenesis is 0.03–10.1% (Karadas, Celikoglu, & Akdag, 2014; Nordgarden, Jensen, & Storhaug, 2002; Rolling & Poulsen, 2001). Tooth agenesis may be isolated or present as part of a syndrome. There are more than 150 syndromes related to tooth agenesis according to the Online Mendelian Inheritance in Man (OMIM) database (Yin & Bian, 2015).

Incontinentia pigmenti (IP; OMIM#308300) is a rare X-linked dominant genetic disorder that affects the skin, hair, teeth, nails, and central nervous system (Ardelean & Pope, 2006; Landy & Donnai, 1993). IP was first reported by Garrod in 1906 (Minic, Trpinac, Gabriel, Gencik, & Obradovic, 2013; Scheuerle & Ursini, 1993; Swinney, Han, & Karth, 2015). The incidence of IP is 1–2 per 1 million in the live births (www.orpha.net/). Roughly, 30–50% of IP patients exhibit tooth agenesis or tooth/oral anomalies (Minic et al., 2013). Approximately 70% of IP cases have *IKBKG* mutations (Fusco et al., 2008). The published data reports that 60–80% of cases have a recurrent deletion of

exon 4–10 of *IKBKG* (Fusco et al., 2014). Other small mutations are concentrated in exon 10 of *IKBKG* (Fusco et al., 2008).

NEMO, also known as I kappa B kinase kinase γ (IKKγ), is coded by the *IKBKG* gene. NEMO acts as the regulatory subunit of the IKK complex and a core component of the canonical NF-κB signalling pathway (Zhang, Lenardo, & Baltimore, 2017). NF-κB regulates various physiological functions, including immune responses, cell apoptosis and survival, and organ development (Ghosh & Hayden, 2008). In the resting state, NF-κB is confined to the cytoplasm as it interacts with inhibitor of NF-κB (IκB) proteins. Under stimuli, canonical NF-κB is activated and is translocated to the nucleus through NEMO-mediated activation of the IKK complex (Zhang et al., 2017). Mutations in *IKBKG* impair transduction of the NF-κB signalling pathway and cause IP, immunodeficiency, or anhidrotic ectodermal dysplasia with immunodeficiency syndrome (Maubach, Schmadicke, & Naumann, 2018). Tooth agenesis is also a common symptom of IP and ˜30% of cases present with tooth agenesis (Swinney et al., 2015).

In this study, we identified a novel nonsense *IKBKG* mutation (c.924 C > G, p.Tyr308*) in a female Chinese patient with IP.

2. Materials and methods

2.1. Participants

The participants were referred from the Department of Prosthodontics, Peking University School and Hospital of Stomatology. The proband was a 15-year-old Chinese female patient receiving orthodontic treatment. Subsequently, her parents were also included in this research. This study was conducted with the approval of the Ethics Committee of Peking University School and the Hospital of Stomatology. Written informed consent for DNA analyses and the reproduction of photographs was obtained from all participants.

2.2. Reagents and antibodies

Lipofectamine 3000 Transfection Reagent was obtained from Thermo Fisher Scientific (St. Louis, MO, USA). Total RNA was isolated using TRIzol® reagent (Thermo Fisher Scientific, Carlsbad, CA, USA) from proband gingival tissue and converted to complementary DNA (cDNA) using GoScriptTM Reverse Transcriptase (Promega Corporation, Madison, WI, USA). The following antibodies were obtained from Santa Cruz Biotechnology (Dallas, TX, USA): anti-NEMO, anti-p65, and anti-HA. Anti-SHARPIN, anti-IKKα, anti-IKKβ, anti-HOIL-1, anti-HOIP, anti-MYC, anti-FLAG, and anti-TRAF6 were purchased from the Proteintech Group (Rosemont, IL, USA). Bound antibodies were visualised with horseradish peroxidase (HRP)-conjugated goat anti-mouse IgG light chain-specific antibody (Abbkine, Redlands, CA, USA) or HRP-conjugated mouse anti-rabbit IgG light chain-specific antibody (Proteintech Group) and an enhanced chemiluminescence kit (Proteintech Group).

2.3. Plasmid construction

The wild-type human NEMO (WT-NEMO) expression plasmid, which contains the full long-coding sequence in the pcDNA3.0-HA vector was a gift from Kunliang Guan (Addgene, Plasmid #13512). The mutant NEMO (MU-NEMO) expression plasmid was constructed by site-directed mutagenesis through PCR as previously described (Lee, Shin, Ryu, Kim, & Ryu, 2010). The following primers were used for mutagenesis: forward, 5′-CCAGGCGGATATCTAGAAGGCGGACTTCCAG-3′; and reverse, 5′-CTGGAAGTCCGCCTTCTAGATATCCGCCTGG-3′.

The additional plasmids used, including MYC-IKKα (Plasmid #19739), FLAG-IKKβ (Plasmid #15465), FLAG-TRAF6 (Plasmid #21624), HA-K63 ubiquitin (Plasmid #17606), MYC-SHARPIN (Plasmid #50014), FLAG-HOIP (Plasmid #50015), and FLAG-HOIL-1 (Plasmid #50016) were obtained from Addgene (Watertown, MA, USA).

2.4. Mutation detection

Genomic DNA was isolated from peripheral blood using the Tiangen DNA Mini-Kit (Tiangen, Beijing, China), according to the manufacturer's instructions. The pseudogene *IKBKG* has > 99% identity with *IKBKG* for exons 3–10 (Frans et al., 2018). Due to the pseudogene, routine direct-sequencing was insufficient to detect mutations in *IKBKG*. Long-range PCR amplified exon 2–10 in *IKBKG*, which has distinct mutations from the pseudogene (Zeevi et al., 2013). Exons 2–10 was amplified by long-range PCR using the primers, forward: 5′- TCG TCAGCAGGCAATAGTTAGTTGGTTGA-3′ and reverse: 5′- TATGCCAAA GATACGCACGACTAATGCAC-3′, after which a secondary PCR was performed for exon 8 because of the existence of a highly homologous pseudogene. The primers used to amplify exon 8 were as follows: forward, 5′-CGAGGAATGCAGCTGGAAGA-3′ and reverse, 5′-CTCATGTCC TCGATCCTGGC-3′. Total RNA of the gingival tissue was obtained and converted to cDNA through reverse transcription-PCR. The DNA and cDNA of the proband were amplified and sequenced (TSINGKE Biological Technology, Beijing, China).

2.5. Generation of IKBKG-deficient HEK293T cells

Single-guide RNA (GTTGGATGAATAGGCACCTC) targeting the second exon of *IKBKG* was subcloned into pSpCas9(BB)-2A-Puro (PX459) V2.0, which was a gift from Feng Zhang (Addgene, Plasmid #62988). The plasmid (2 μg/well) was transfected into 6-well plates containing HEK293T cells. At 24 h after transfection, cells were selected with puromycin (5 μg/ml) for 2 days. Individual cell clones were picked and further expanded. Expression of NEMO was determined by immunoblotting.

### 2.6. NF-κB reporter gene activity

IKBKG-deficient HEK293T cells were transfected with an empty vector, wild-type, or mutant NEMO plasmid (400 ng/well) in 24-well plates using Lipofectamine 3000 reagent according to the manufacturer's instructions. The NF-κB and Renilla luciferase reporter vectors (300 ng/well) were co-transfected. At 24 h after transfection, cells were stimulated with 100 ng/ml human lipopolysaccharide (1 μg/ml) for 6 h. Firefly and Renilla luciferase activities were then measured using the Dual Reporter Assay system (Promega Corporation) according to the manufacturer's instructions.

2.7. Analysis of NF-κB activation

IKBKG-deficient HEK293T cells were cultured in high-glucose Dulbecco's modified Eagle's medium (Invitrogen Life Technologies) supplemented with 10% foetal bovine serum and 2 mM L-glutamine. Wild-type or mutant NEMO plasmid (3 μg/dish) was transiently transfected into *IKBKG*-deficient HEK293T cells using Lipofectamine 3000 reagent in 100 mm dishes. To analyse the functional changes of the truncated mutation, lipopolysaccharide (1 μg/ml; Sigma-Aldrich) was used to stimulate cells for 0, 5, 15, and 30 min at 48 h after transfection.

2.8. Immunoprecipitation

HEK293T cells were transiently transfected with wild-type or mutant NEMO plasmids/various plasmids (3 μg/dish) in 100 mm dishes. Cells were lysed with Native Lysis Buffer (Solarbio, Beijing, China), 1 mM phenylmethanesulfonyl fluoride, and a mixture of 1 mM protease inhibitors (Cwbiotech Beijing, China) at 24 h after transfection. Immunoprecipitation was performed using Protein A/G Magnetic Beads (MedChemExpress, Monmouth Junction, NJ, USA), followed by immunoblotting.
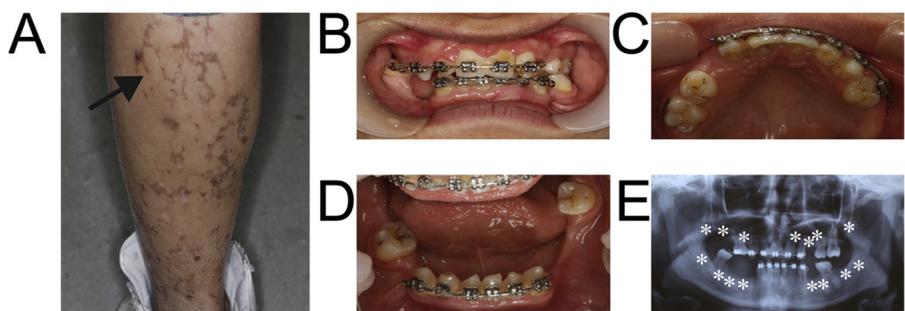
Fig. 1. Clinical phenotypes of the proband.
(A) Reticular hyperpigmentation in the proband (black arrows). (B−D) Intraoral photographs of the proband. (E) Panoramic radiographs of the proband (*indicates missing teeth). (F) Schematic representation of congenitally missing teeth of the proband (black squares indicate missing teeth).
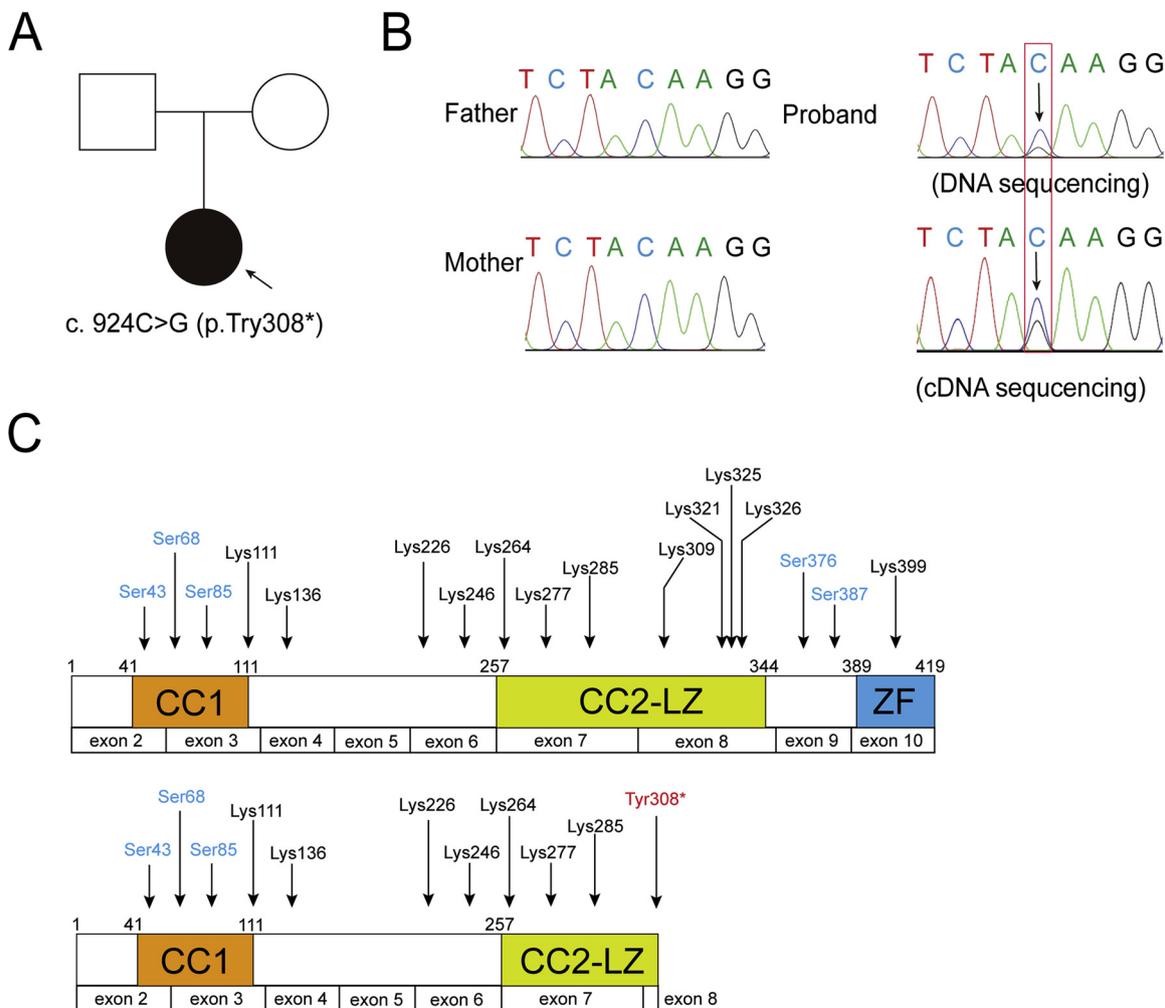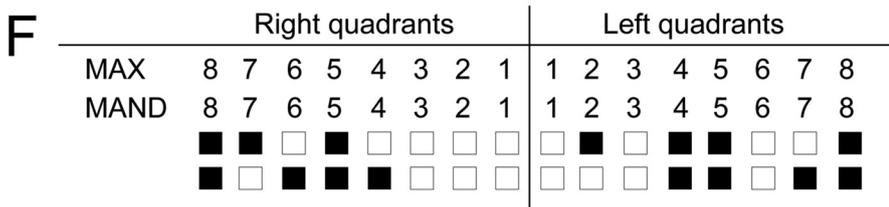
Fig. 2. Mutation analyses of the *IKBKG* gene.
(A) Pedigree chart of the proband. (B) DNA and cDNA sequencing of exon 8 of the *IKBKG* gene of the proband. A *de novo* nonsense mutation, c.924C > G, was present in the proband but not in the patient's parents. (C) Schematic diagram of wild-type and mutant NEMO. Blue, black and red indicate phosphorylation sites, ubiquitination sites and the mutation site of *IKBKG*, respectively. Abbreviations: CC1, coil-coiled domain; LZ, leucine zipper; ZF, zinc finger.

A

B
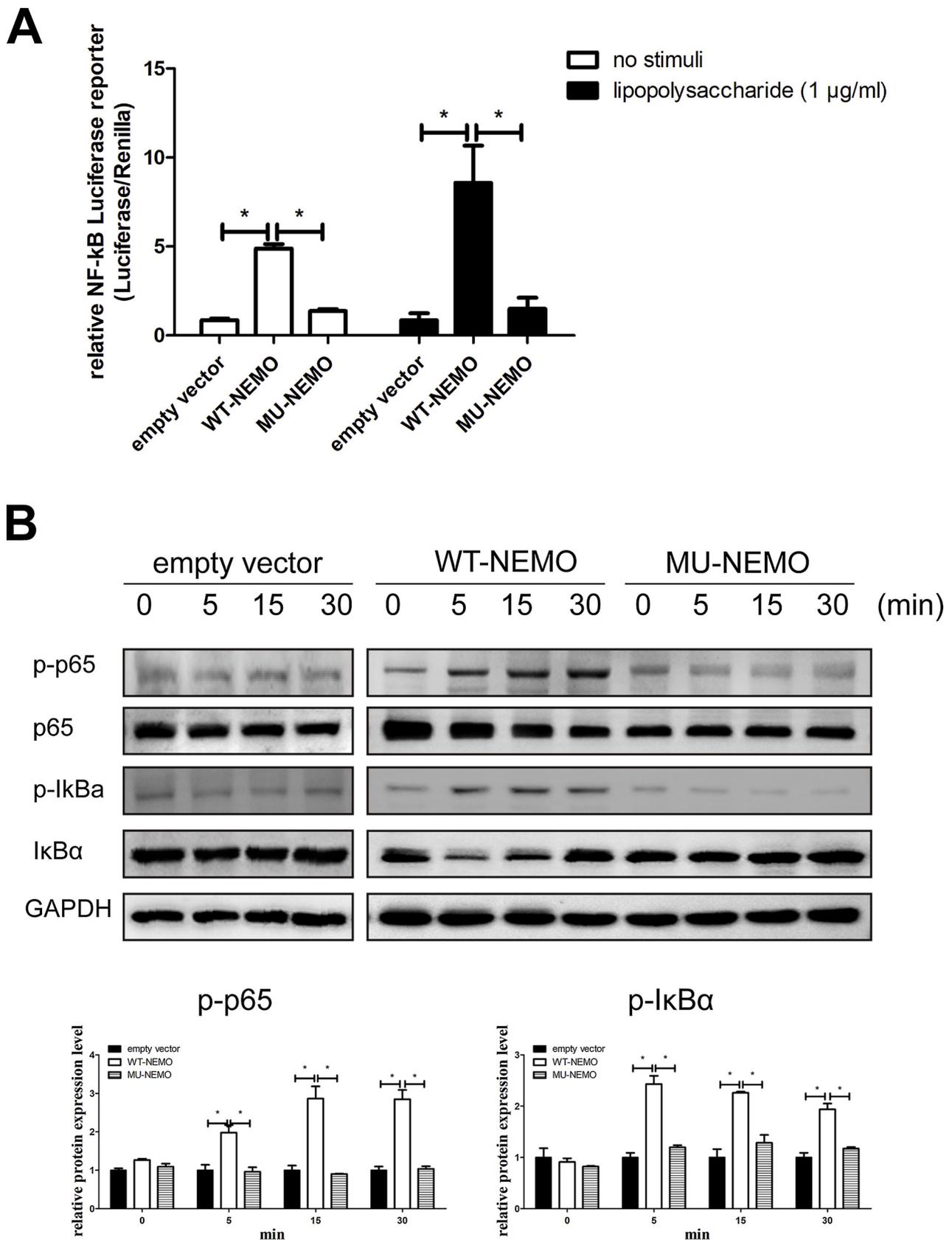
Fig. 3. Functional analysis of truncated NEMO.

(A) A dual-luciferase reporter assay showing NF-κB inactivity in truncated NEMO stimulated by lipopolysaccharide. The bar charts show the quantification of relative fluorescence intensities (mean ± SD, n = 3, $*p < 0.05$). (B) Immunoblot analysis showed that overexpression of the mutant protein resulted in severely impaired phosphorylation of p65 and degradation of IκBα following lipopolysaccharide stimulation. The bar charts show the quantification of band intensities (mean ± SD, n = 3, $*p < 0.05$).

A

B
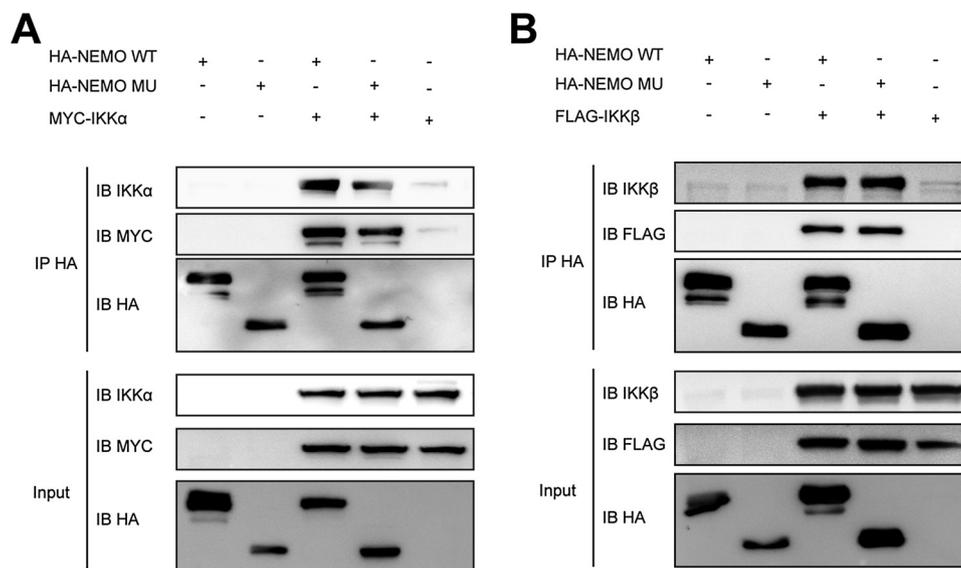
Fig. 4. Truncated NEMO integrated into IKKα and IKKβ.
Co-transfection of IKKα or IKKβ plasmids into HEK293T cells with wild-type or truncated NEMO constructs. Immunoprecipitation and immunoblotting analyses revealed that truncated NEMO interacts with IKKα and IKKβ.

2.9. Statistical analyses

Statistical analyses were performed using SPSS version 13.0 software (SPSS Inc., Chicago, IL, USA). The data are presented as the mean and standard deviation (mean $\pm$ SD) with error bars, and analysed by one-way analysis of variance followed by Tukey's HSD test; $p < 0.05$ was taken to indicate statistical significance. Experiments were carried out in triplicate.

3. Results

3.1. Clinical findings

General examination showed the proband manifested mild symptoms of ectodermal dysplasia, such as thin eyebrows, hypofunction of sweat and salivary secretions, and deposition of reticular pigment in the calf (Fig. 1A). Clinical and radiographic examination of the oral cavity revealed 15 congenitally missing teeth, including the third molars (15, 17, 18, 22, 23, 24, 28, 34, 35, 37, 38, 44, 45, 46 and 48). Furthermore, 31, 32, 41 and 42 were conical (Fig. 1B–E). Her parents were asymptomatic and did not show any family history of tooth agenesis or other genetic diseases.

3.2. Mutation analysis

Using long-range PCR and Sanger sequencing, a novel nonsense heterozygous mutation (c.924C > G, p.Tyr308*) was detected in exon 8 of *IKBKG* in the proband. The patient's parents were asymptomatic (Fig. 2A). Analysis of the mutation showed a heterozygous C to G transition at nucleotide 924 (c.924C > G) of the coding sequence in exon 8 of the *IKBKG* gene (Fig. 2B). The mutation c.924C > G changed the tyrosine (TAC) residue at 308 to a stop codon (TAG) (p.Tyr308*), resulting in truncation of NEMO and partial loss of the coil-coiled 2-leucine zipper domain and zinc finger domain (Fig. 2C).

3.3. Functional analysis of truncated NEMO

A dual-luciferase reporter assay showed that NF-κB activity was higher in WT-NEMO than in both the empty vector and MU-NEMO ($p < 0.05$); also, there was no difference between the latter two (Fig. 3A). This indicated that truncated NEMO was unable to activate NF-κB when stimulated by lipopolysaccharide. The mutation (p.Tyr308*) inhibited NF-κB activity completely. As observed in *IKBKG*-deficient cells, overexpression of the mutant protein (p.Tyr308*) exhibited severely impaired phosphorylation of p65 and degradation of IκBα following lipopolysaccharide stimulation (Fig. 3B). Phosphorylation of p65 and IκBα was higher in WT-NEMO than in both the empty vector and MU-NEMO at 5, 15 and 30 min ($p < 0.05$). Therefore, c.924C > G is a loss-of-function mutation that inactivates the NEMO protein and impairs the NF-κB signalling pathway.

3.4. Truncated NEMO formed an IKK complex

Following co-transfection of HEK293T cells with wild-type or mutant NEMO plasmid and MYC-IKKα or FLAG-IKKβ plasmid, immunoprecipitation and immunoblotting analyses revealed that the truncated NEMO protein was assembled as part of the IKK complex with IKKα or IKKβ (Fig. 4A and B).

3.5. Truncated NEMO suppressed K63-linked polyubiquitination

TRAF6 is a specific ubiquitin-ligase mediated K63-linked polyubiquitination of NEMO. To detect K63-linked polyubiquitination of NEMO, wild-type or mutant NEMO plasmid and FLAG-TRAF6 or HA-K63 ubiquitin plasmid were co-transfected to HEK293T cells. Immunoprecipitation and immunoblotting analyses revealed that truncated NEMO did not interact with TRAF6 to the same extent as wild-type NEMO (Fig. 5A). K63-linked polyubiquitination was limited with truncated NEMO in immunoprecipitation and immunoblotting analyses (Fig. 5B).

3.6. Truncated NEMO suppressed linear polyubiquitination by failing to interact with HOIL-1 and SHARPIN

Linear ubiquitin chain assembly complex (LUBAC), consisted by HOIP, HOIL-1, and SHARPIN, catalysed linear polyubiquitination of NEMO. To assess the linear polyubiquitination of wild-type and truncated NEMO proteins, the 3 LUBAC subunits (HOIP, HOIL-1, and SHARPIN) and wild-type and truncated NEMO plasmids were co-transfected into HEK293T cells. Immunoprecipitation and immunoblotting analyses showed a defect in linear polyubiquitination of the truncated NEMO protein (Fig. 5C).
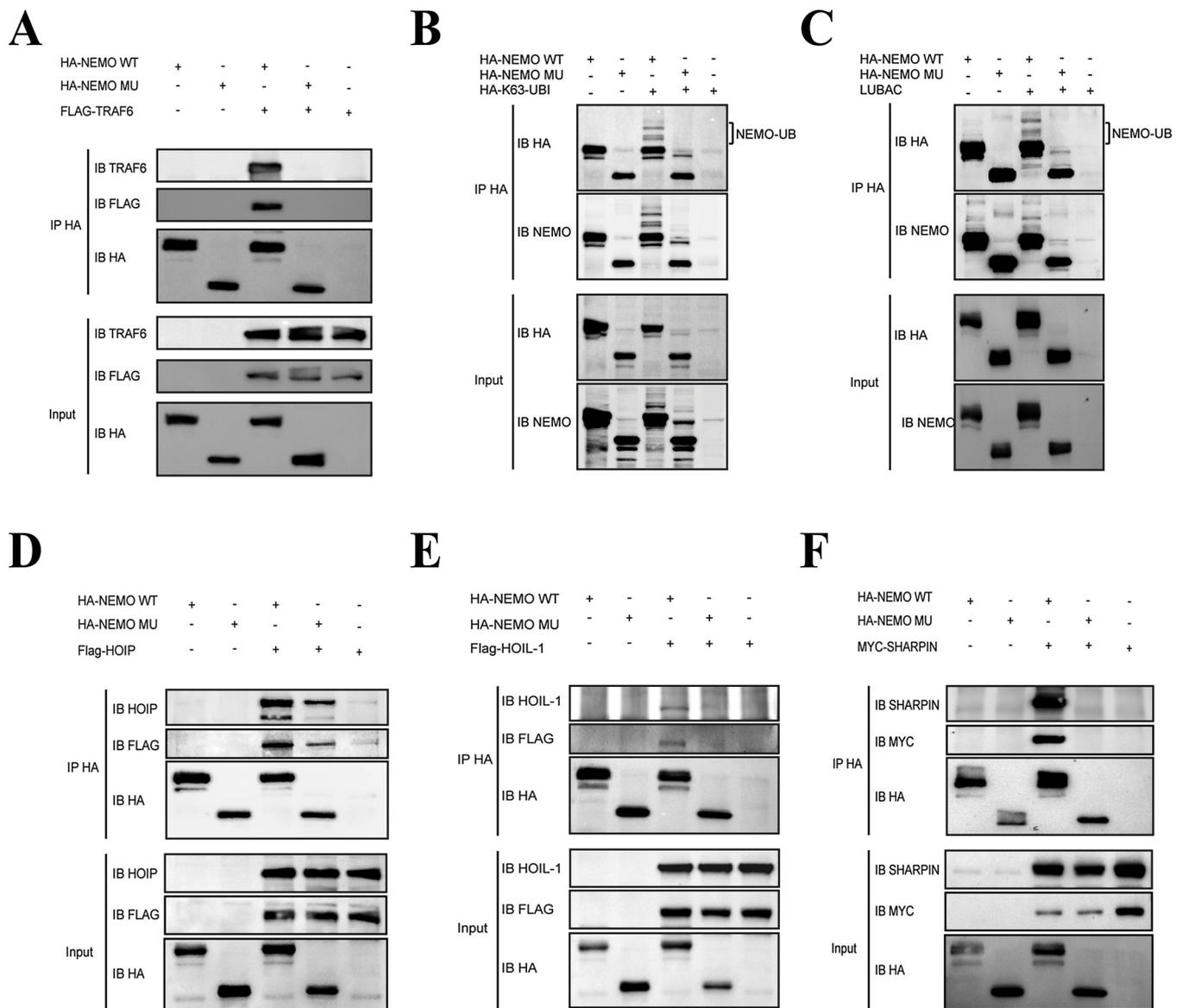
Fig. 5. Mutation inhibited ubiquitination of NEMO.
(A and B) Wild-type and truncated NEMO plasmids were transfected into HEK293T cells with a FLAG-TRAF6 (A) or HA-K63 ubiquitin plasmid (B). Immunoprecipitation and immunoblotting analyses revealed that truncated NEMO loses its interaction with TRAF6 (A) and K63-linked polyubiquitination was decreased in the mutant NEMO (B). (C) Three subunits of LUBAC (FLAG-HOIP, FLAG-HOIL-1 or MYC-SHARPIN) with the wild-type or mutant NEMO plasmid were co-transfected in HEK293T cells. Immunoprecipitation and immunoblotting analyses demonstrated linear polyubiquitination was reduced in truncated NEMO. (D–F) Interactions between LUBAC subunits and wild-type or truncated NEMO. FLAG-HOIP (D), FLAG-HOIL-1 (E), or MYC-SHARPIN (F) plasmids were transfected into HEK293T cells with wild-type or truncated NEMO plasmid, respectively. Immunoprecipitation and immunoblotting analyses demonstrated that wild-type NEMO interacted with all LUBAC subunits; however, the mutant NEMO did not interact with HOIL-1 or SHARPIN.

To assess the effect of each subunit of LUBAC, wild-type and truncated NEMO plasmids were co-transfected into HEK293T cells. Immunoprecipitation and immunoblotting analyses revealed that wild-type NEMO protein interacted with all of the subunits of LUBAC (HOIL-1, HOIP, and SHARPIN). By contrast, the truncated NEMO interacted with HOIP but not with SHARPIN or HOIL-1 (Fig. 5D–F).

4. Discussion

We identified a novel nonsense mutation in the *IKBKG* gene in a Chinese female IP patient. The nonsense mutation (c.924C > G, p.Tyr308*) resulted in a loss of the coil-coiled 2-leucine zipper and zinc finger domains of NEMO.

IKBKG mutations result in IP, which is frequently accompanied by various anomalies, including those of the teeth, eyes, hair, nails, or central nervous system (Minic, Trpinac, & Obradovic, 2014). However, the clinical characteristics of tooth agenesis with *IKBKG* mutations remain unclear because *IKBKG* mutations can cause abortion or early death of infants (Conte et al., 2014). Minic et al. identified that the most common dental anomalies in IP were tooth shape abnormity and oligodontia (36.42% and 31.22%, respectively) (Minic et al., 2013, 2014). Roberts et al. identified the deletion 1182_1183delTT in the *IKBKG* gene in a young male, which caused erupted conical teeth (Roberts et al., 2010). In 2011, Hadj-Rabia et al. identified hypodontia in seven teeth of a female IP patient (Hadj-Rabia et al., 2011). In 2012, Naoki et al. reported a 10-year-old girl and her mother who manifested IP with agenesis of the upper anterior teeth (Oiso et al., 2012). In the present study, the proband had 15 congenitally missing permanent teeth (including four third molars) and conical-shaped mandibular central and lateral incisors. We also detected another IP patient

carrying a common exon 4–10 deletion in *IKBKG*. The dental phenotype of the patient was the loss of 19 permanent teeth (12, 14, 15, 17, 18, 22, 24, 25, 27, 28, 31, 32, 34, 38, 41, 44, 45, 47 and 48), with the majority of these being posterior teeth; primary teeth (65, 74, and 85) were retained (Figs. S1 and S2). This suggests that posterior teeth are at greater risk in IP.

Deletion of exon 4–10 of *IKBKG* is most common in IP patients. *In vitro* functional analysis demonstrated that genomic rearrangement inactivated NF-κB, although it retained its interaction with IKKα and IKKβ (Smahi et al., 2000). The nonsense mutation in the proband has not been reported previously. Mutation analysis revealed that c.924C > G impaired the major domain of NEMO (Fig. 2C). This was confirmed by the dual-luciferase reporter assay and immunoblotting (Fig. 3). K63-linked polyubiquitin chains bind the zinc finger domain of NEMO and this is important in activation of the IKK complex (Laplantine et al., 2009). Sebban-Benin et al. reported that the mutation A323P in the zinc finger domain of NEMO was responsible for severe IP. A323P inhibited K63-linked polyubiquitination of NEMO by disturbing the TRAF6/NEMO interaction (Sebban-Benin et al., 2007). Immunoprecipitation and immunoblotting analyses revealed that K63-linked polyubiquitin chains were prevented from binding truncated NEMO by the inactivation of TRAF6, which was not able to interact with truncated NEMO (Fig. 5A and B). This indicates that truncated NEMO inhibits K63-linked polyubiquitination. Recently, a new type of ubiquitin chain, namely a linear polyubiquitin chain, was identified (Ikeda, 2015). Linear polyubiquitination of NEMO was shown to be essential to activate NF-κB (Niu, Shi, Iwai, & Wu, 2011). Linear polyubiquitin chains demonstrated high-affinity binding to NEMO and suppression of the LUBAC/NEMO interaction, which decreased NF-κB activity (Ikeda, 2015; de Jong, Liu, Chen, & Alto, 2016). Linear polyubiquitination of NEMO is mediated by LUBAC, which binds and catalyses the linear polyubiquitination of NEMO at Lys285 and Lys309, located in the coil-coiled 2-leucine zipper domain (Ebner, Versteeg, & Ikeda, 2017; Hooper, Jackson, Coughlin, Coon, & Miyamoto, 2014; Ikeda, 2015; Tokunaga et al., 2009). The Tyr308* mutation results in loss of one of the linear polyubiquitination sites (Fig. 2C). Furthermore, immunoprecipitation assays revealed that wild-type NEMO interacted with all of the subunits of LUBAC. By contrast, truncated NEMO was only able to interact with HOIP, but not with HOIL-1 and SHARPIN (Fig. 5D–F). Recently, Elodie et al. reported that a splicing mutation led to NEMO losing its ability to interact with SHARPIN, which inhibits linear polyubiquitination of NEMO and leads to IP (Bal et al., 2017). This mutation also disrupts the polyubiquitination of NEMO. Similarly, the truncated NEMO does not interact with SHARPIN. Additionally, Tyr308* perturbs the NEMO/HOIL-1 interaction, which is important for LUBAC catalysing linear ubiquitination of NEMO. Recently, paracaspase MALT-1 has been reported to decrease NF-κB activation by impairing the HOIL-1/NEMO interaction through cleavage of HOIL-1 by MALT-1, resulting in disruption of linear polyubiquitination of NEMO (Klein et al., 2015).

In conclusion, we identified a novel heterozygous nonsense mutation (c.924C > G; p.Tyr308*) in *IKBKG* in an IP patient with syndromic tooth agenesis in the Chinese population. This research enriches our knowledge of the mutation and phenotype spectra of the *IKBKG* gene. Furthermore, the functional analyses suggest that the mutation impaired NF-κB activation. However, the precise role of *IKBKG* in tooth agenesis remains to be clarified in further studies.

Conflicts of interests

None of the authors of the present study has a conflict of interest to declare.

Acknowledgments

Appendix A. Supplementary data

Supplementary material related to this article can be found, in the online version, at doi:https://doi.org/10.1016/j.archoralbio.2019.03.013.

References

Ardelean, D., & Pope, E. (2006). Incontinentia pigmenti in boys: A series and review of the literature. *Pediatric Dermatology, 23*(6), 523–527. https://doi.org/10.1111/j.1525-1470.2006.00302.x.

Bal, E., Laplantine, E., Hamel, Y., Dubosclard, V., Boisson, B., Pescatore, A., ... Smahi, A. (2017). Lack of interaction between NEMO and SHARPIN impairs linear ubiquitination and NF-kappaB activation and leads to incontinentia pigmenti. *The Journal of Allergy and Clinical Immunology, 140*(6), 1671–1682. https://doi.org/10.1016/j.jaci.2016.11.056 e1672.

Conte, M. I., Pescatore, A., Paciolla, M., Esposito, E., Miano, M. G., Lioi, M. B., ... Ursini, M. V. (2014). Insight into IKBKG/NEMO locus: Report of new mutations and complex genomic rearrangements leading to incontinentia pigmenti disease. *Human Mutation, 35*(2), 165–177. https://doi.org/10.1002/humu.22483.

de Jong, M. F., Liu, Z., Chen, D., & Alto, N. M. (2016). Shigella flexneri suppresses NF-kappaB activation by inhibiting linear ubiquitin chain ligation. *Nature Microbiology, 1*(7), 16084. https://doi.org/10.1038/nmicrobiol.2016.84.

Ebner, P., Versteeg, G. A., & Ikeda, F. (2017). Ubiquitin enzymes in the regulation of immune responses. *Critical Reviews in Biochemistry and Molecular Biology, 52*(4), 425–460. https://doi.org/10.1080/10409238.2017.1325829.

Frans, G., Meert, W., Van der Werff, Ten, Bosch, J., Meyts, I., Bossuyt, X., ... Hestand, M. S. (2018). Conventional and single-molecule targeted sequencing method for specific variant detection in IKBKG while bypassing the IKBKGP1 pseudogene. *The Journal of Molecular Diagnostics: JMD, 20*(2), 195–202. https://doi.org/10.1016/j.jmoldx.2017.10.005.

Fusco, F., Paciolla, M., Conte, M. I., Pescatore, A., Esposito, E., Mirabelli, P., ... Ursini, M. V. (2014). Incontinentia pigmenti: Report on data from 2000 to 2013. *Orphanet Journal of Rare Diseases, 9*, 93. https://doi.org/10.1186/1750-1172-9-93.

Fusco, F., Pescatore, A., Bal, E., Ghoul, A., Paciolla, M., Lioi, M. B., ... Ursini, M. V. (2008). Alterations of the IKBKG locus and diseases: An update and a report of 13 novel mutations. *Human Mutation, 29*(5), 595–604. https://doi.org/10.1002/humu.20739.

Ghosh, S., & Hayden, M. S. (2008). New regulators of NF-kappaB in inflammation. *Nature Reviews Immunology, 8*(11), 837–848. https://doi.org/10.1038/nri2423.

Hadj-Rabia, S., Rimella, A., Smahi, A., Fraitag, S., Hamel-Teillac, D., Bonnefont, J. P., ... Bodemer, C. (2011). Clinical and histologic features of incontinentia pigmenti in adults with nuclear factor-kappaB essential modulator gene mutations. *Journal of the American Academy of Dermatology, 64*(3), 508–515. https://doi.org/10.1016/j.jaad.2010.01.045.

Hooper, C., Jackson, S. S., Coughlin, E. E., Coon, J. J., & Miyamoto, S. (2014). Covalent modification of the NF-kappaB essential modulator (NEMO) by a chemical compound can regulate its ubiquitin binding properties in vitro. *The Journal of Biological Chemistry, 289*(48), 33161–33174. https://doi.org/10.1074/jbc.M114.582478.

Ikeda, F. (2015). Linear ubiquitination signals in adaptive immune responses. *Immunological Reviews, 266*(1), 222–236. https://doi.org/10.1111/imr.12300.

Karadas, M., Celikoglu, M., & Akdag, M. S. (2014). Evaluation of tooth number anomalies in a subpopulation of the North-East of Turkey. *European Journal of Dentistry, 8*(3), 337–341. https://doi.org/10.4103/1305-7456.137641.

Klein, T., Fung, S. Y., Renner, F., Blank, M. A., Dufour, A., Kang, S., ... Overall, C. M. (2015). The paracaspase MALT1 cleaves HOIL1 reducing linear ubiquitination by LUBAC to dampen lymphocyte NF-kappaB signalling. *Nature Communications, 6*, 8777. https://doi.org/10.1038/ncomms9777.

Landy, S. J., & Donnai, D. (1993). Incontinentia pigmenti (Bloch-Sulzberger syndrome). *Journal of Medical Genetics, 30*(1), 53–59.

Laplantine, E., Fontan, E., Chiaravalli, J., Lopez, T., Lakisic, G., Veron, M., ... Israel, A. (2009). NEMO specifically recognizes K63-linked poly-ubiquitin chains through a new bipartite ubiquitin-binding domain. *The EMBO Journal, 28*(19), 2885–2895. https://doi.org/10.1038/emboj.2009.241.

Lee, J., Shin, M. K., Ryu, D. K., Kim, S., & Ryu, W. S. (2010). Insertion and deletion mutagenesis by overlap extension PCR. *Methods in Molecular Biology, 634*, 137–146. https://doi.org/10.1007/978-1-60761-652-8_10.

Maubach, G., Schmadicke, A. C., & Naumann, M. (2018). NEMO links nuclear Factor-kappaB to human diseases: (Trends mol med. 23, 1138-1155; 2017). *Trends in Molecular Medicine.* https://doi.org/10.1016/j.molmed.2018.01.009.

Minic, S., Trpinac, D., Gabriel, H., Gencik, M., & Obradovic, M. (2013). Dental and oral anomalies in incontinentia pigmenti: A systematic review. *Clinical Oral Investigations, 17*(1), 1–8. https://doi.org/10.1007/s00784-012-0721-5.

Minic, S., Trpinac, D., & Obradovic, M. (2014). Incontinentia pigmenti diagnostic criteria update. *Clinical Genetics, 85*(6), 536–542. https://doi.org/10.1111/cge.12223.

Niu, J., Shi, Y., Iwai, K., & Wu, Z. H. (2011). LUBAC regulates NF-kappaB activation upon genotoxic stress by promoting linear ubiquitination of NEMO. *The EMBO Journal, 30*(18), 3741–3753. https://doi.org/10.1038/emboj.2011.264.

Nordgarden, H., Jensen, J. L., & Storhaug, K. (2002). Reported prevalence of congenitally missing teeth in two Norwegian counties. *Community Dental Health, 19*(4), 258–261.

Oiso, N., Kimura, M., Tanemura, A., Tsuruta, D., Itou, T., Suzuki, T., ... Kawada, A. (2012). Blaschkitis-like eruptions with hypodontia and low IkappaB kinase gamma expression. *The Journal of Dermatology, 39*(11), 941–943. https://doi.org/10.1111/j.1346-8138.2011.01493.x.

Roberts, C. M., Angus, J. E., Leach, I. H., McDermott, E. M., Walker, D. A., & Ravenscroft, J. C. (2010). A novel NEMO gene mutation causing osteopetrosis, lymphoedema, hypohidrotic ectodermal dysplasia and immunodeficiency (OL-HED-ID). *European Journal of Pediatrics, 169*(11), 1403–1407. https://doi.org/10.1007/s00431-010-1206-7.

Rolling, S., & Poulsen, S. (2001). Oligodontia in danish schoolchildren. *Acta Odontologica Scandinavica, 59*(2), 111–112.

Scheuerle, A. E., & Ursini, M. V. (1993). Incontinentia pigmenti. In R. A. Pagon, M. P. Adam, H. H. Ardinger, S. E. Wallace, A. Amemiya, L. J. H. Bean, T. D. Bird, N. Ledbetter, H. C. Mefford, R. J. H. Smith, & K. Stephens (Eds.). *GeneReviews(R)*Seattle (WA): University of Washington, Seattle University of Washington, Seattle GeneReviews is a registered trademark of the University of Washington, Seattle. All rights reserved.

Sebban-Benin, H., Pescatore, A., Fusco, F., Pascuale, V., Gautheron, J., Yamaoka, S., ... Courtois, G. (2007). Identification of TRAF6-dependent NEMO polyubiquitination sites through analysis of a new NEMO mutation causing incontinentia pigmenti. *Human Molecular Genetics, 16*(23), 2805–2815. https://doi.org/10.1093/hmg/ddm237.

Smahi, A., Courtois, G., Vabres, P., Yamaoka, S., Heuertz, S., Munnich, A., ... Nelson, D. L. (2000). Genomic rearrangement in NEMO impairs NF-kappaB activation and is a cause of incontinentia pigmenti. The International Incontinentia Pigmenti (IP) Consortium. *Nature, 405*(6785), 466–472. https://doi.org/10.1038/35013114.

Swinney, C. C., Han, D. P., & Karth, P. A. (2015). Incontinentia pigmenti: A comprehensive review and update. *Ophthalmic Surgery, Lasers & Imaging Retina, 46*(6), 650–657. https://doi.org/10.3928/23258160-20150610-09.

Tokunaga, F., Sakata, S., Saeki, Y., Satomi, Y., Kirisako, T., Kamei, K., ... Iwai, K. (2009). Involvement of linear polyubiquitylation of NEMO in NF-kappaB activation. *Nature Cell Biology, 11*(2), 123–132. https://doi.org/10.1038/ncb1821.

Yin, W., & Bian, Z. (2015). The gene network underlying hypodontia. *Journal of Dental Research, 94*(7), 878–885. https://doi.org/10.1177/0022034515583999.

Zeevi, D. A., Renbaum, P., Ron-El, R., Eldar-Geva, T., Raziel, A., Brooks, B., ... Altarescu, G. (2013). Preimplantation genetic diagnosis in genomic regions with duplications and pseudogenes: Long-range PCR in the single-cell assay. *Human Mutation, 34*(5), 792–799. https://doi.org/10.1002/humu.22298.

Zhang, Q., Lenardo, M. J., & Baltimore, D. (2017). 30 years of NF-kappaB: A blossoming of relevance to human pathobiology. *Cell, 168*(1-2), 37–57. https://doi.org/10.1016/j.cell.2016.12.012.